

Table S1: The ^1H NMR data of the HI and IA.

Comp.	δ (ppm)	
	Δ (ppm) map (existing)	δ (ppm) map (analyzed)
HI		
δ (ppm)		
IA	Δ (ppm) map (existing)	δ (ppm) map (analyzed)

*ppm: part per million, δ =shift value of ^1H NMR

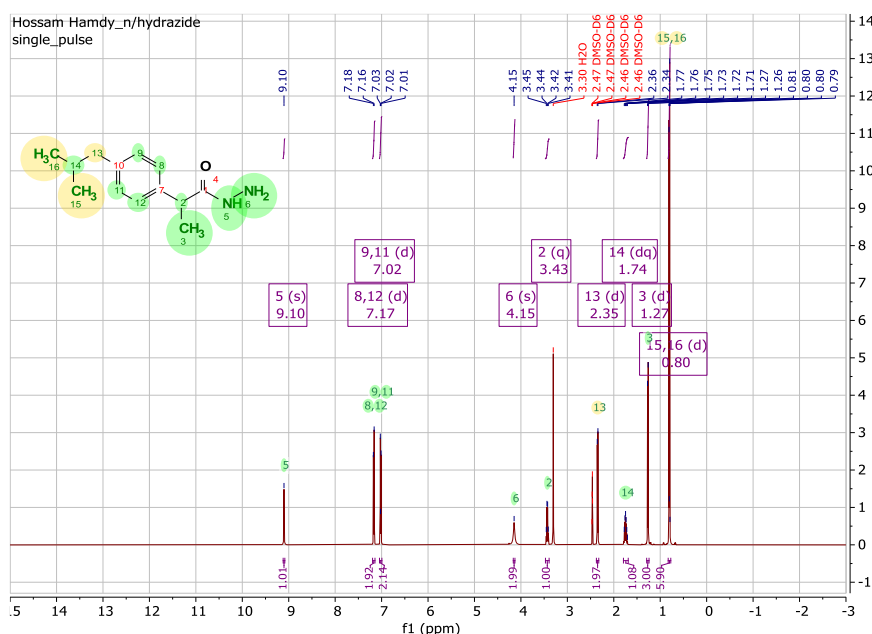


Figure S1: ^1H NMR spectrum of Hydrazide Ibuprofen (HI).

Chromatogram

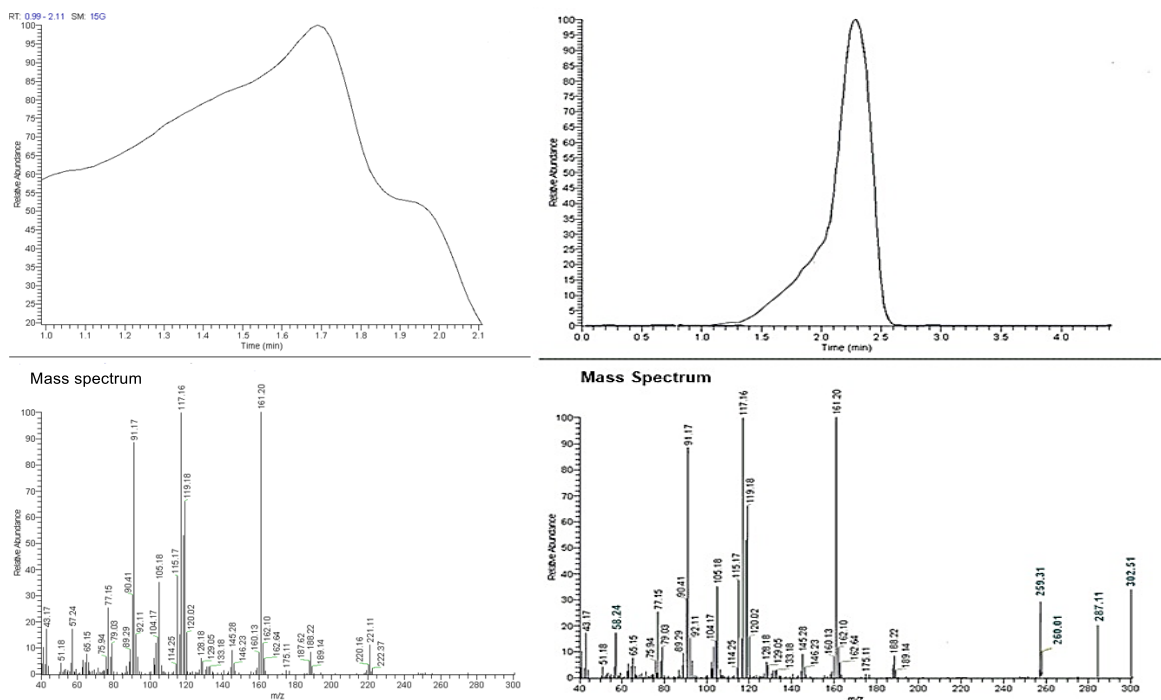
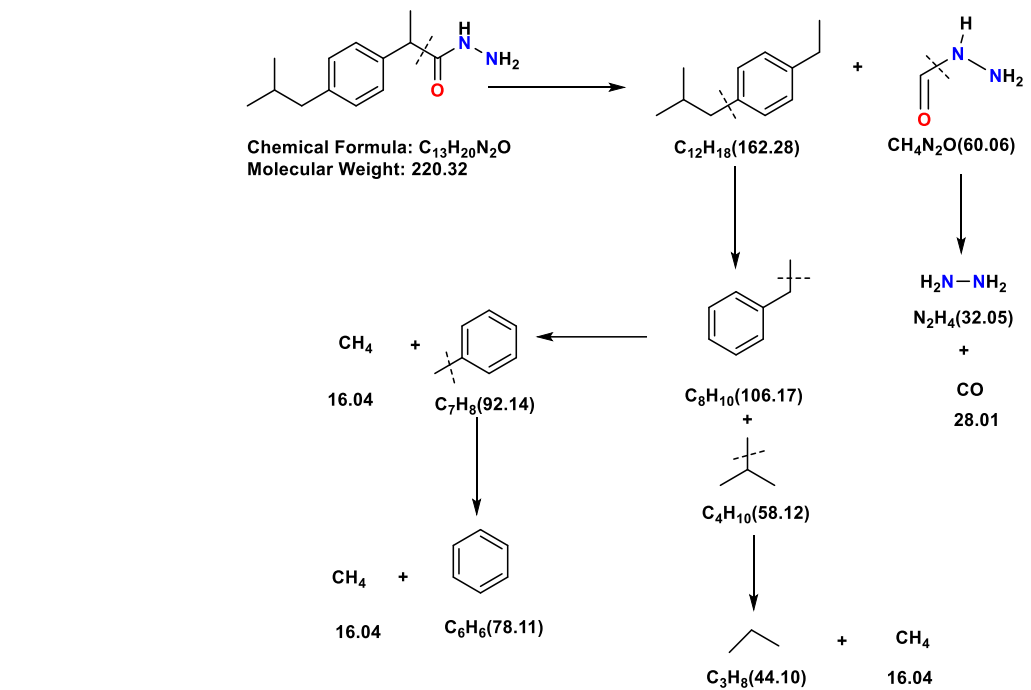
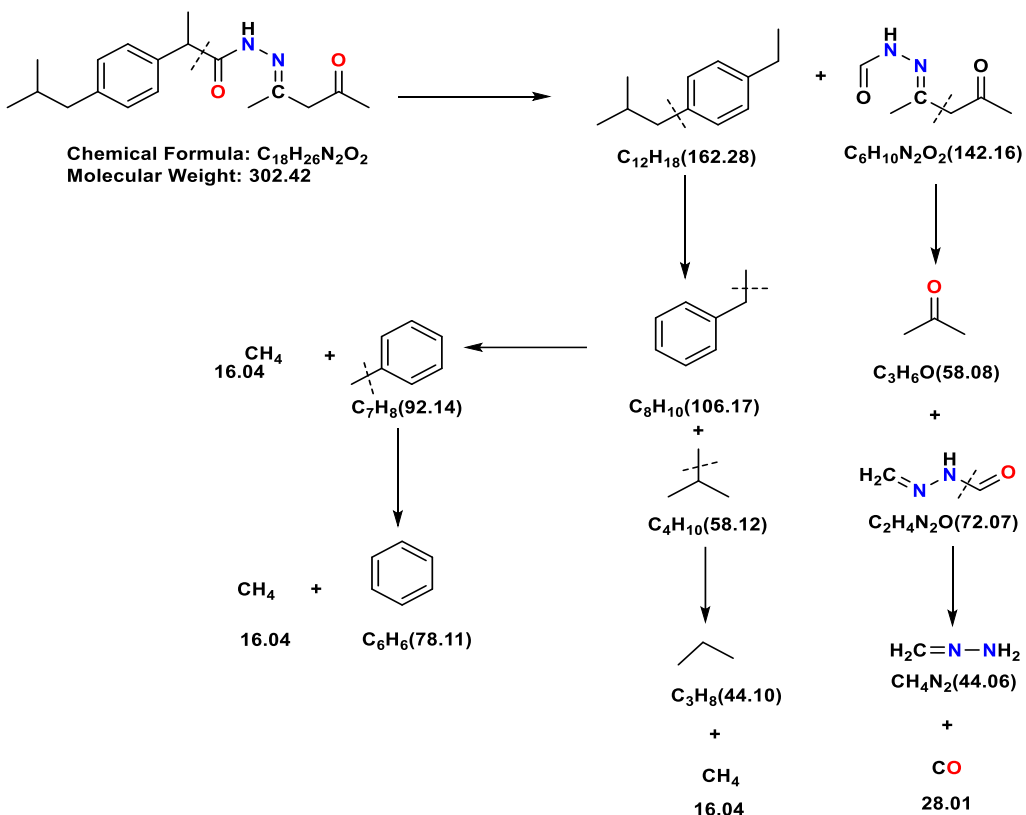


Figure S2: Chromatogram and mass spectrum of **HI** (on Left) and **IA** (on Right).



Scheme S1: The chromatogram of pathway fragmentation of Hydrazide Ibuprofen (**HI**).



Scheme S2: The chromatogram of pathway fragmentation of **IA** ligand.

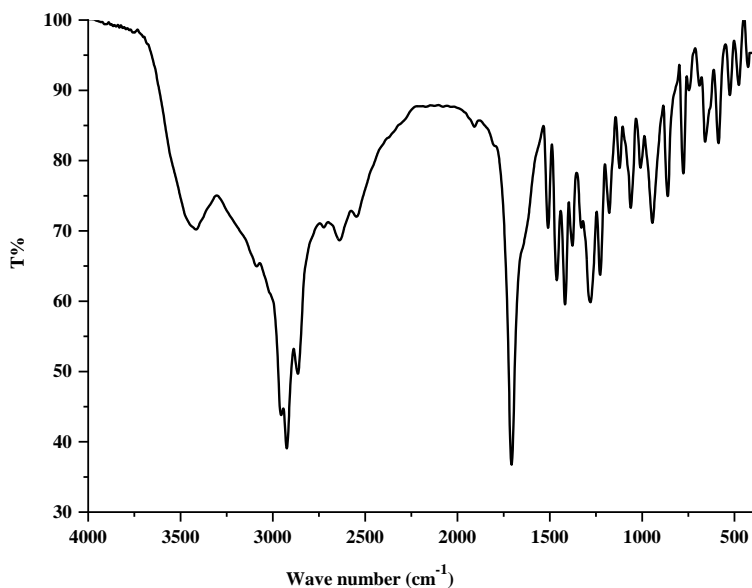


Figure S3: FTIR spectrum of the parent drug (**ibuprofen**).

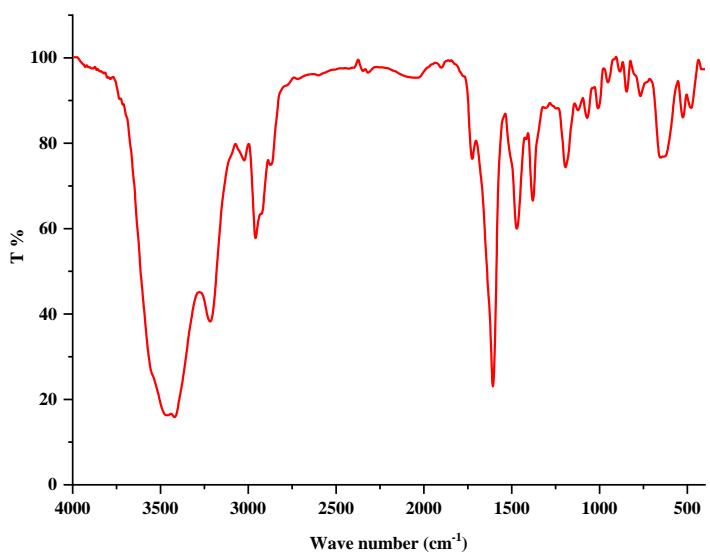


Figure S4: FTIR spectrum of the ligand **IA**.

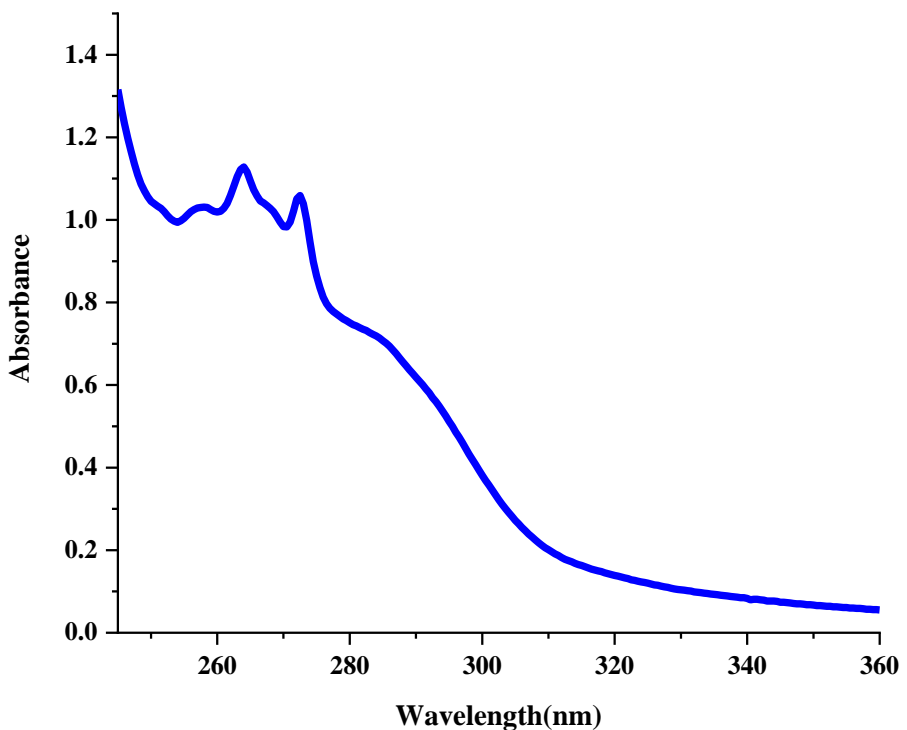


Figure S5: UV-Vis. spectrum of the ligand **IA**.

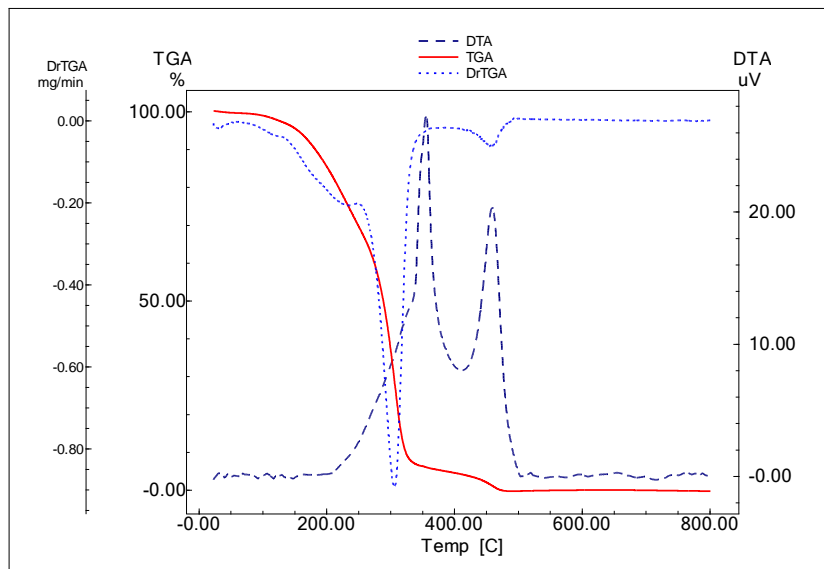


Figure S6: Thermal decomposition of Schiff base IA.

Table S2: TG/DTG and DTA data of IA.

<i>Compound</i>	<i>Temp. range</i> °C	<i>DTA peak</i>		<i>Peak type</i>	<i>ΔH (KJ/g)</i>	<i>Process</i>
		<i>temp.</i> °C				
IA	111.7-136	130		Endo	0.017	Ligand decomposition
	346-367	355		Exo	-0.401	Ligand decomposition
	436-480	460		Exo	-0.0147	Final decomposition

<i>Compound</i>	<i>Temp. range</i> °C	<i>DTG</i> <i>Temp.</i> °C	<i>Mass loss %</i>		<i>Process</i>	<i>expected products</i>
			<i>Found</i>	<i>Calculated</i>		
IA	261-321	306	96.61	95.04	Ligand decomposition	0.95 IA
	443-473	458	3.68	4.96	Final decomposition	0.50 IA

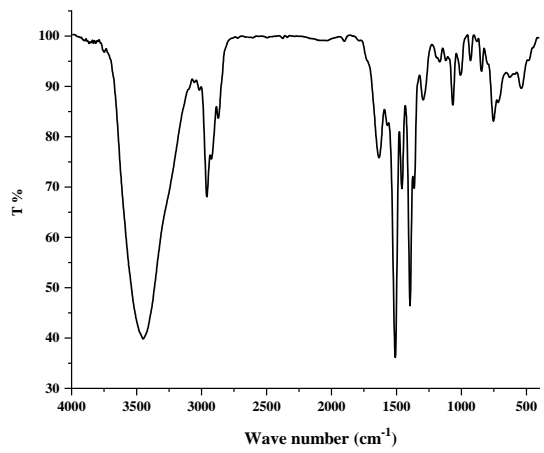


Figure S7: FTIR spectrum of $[\text{Cu}(\text{IA})\text{Cl}_2\cdot\text{H}_2\text{O}]6\text{H}_2\text{O}$.

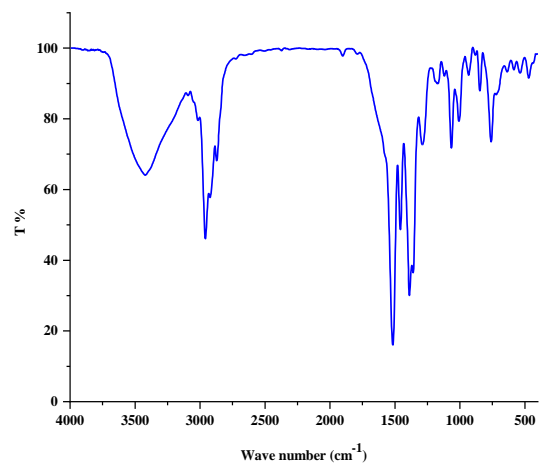


Figure S8: FTIR spectrum of $[\text{Ni}(\text{IA})(\text{H}_2\text{O})_3]\text{Cl}_2\cdot\text{H}_2\text{O}$.

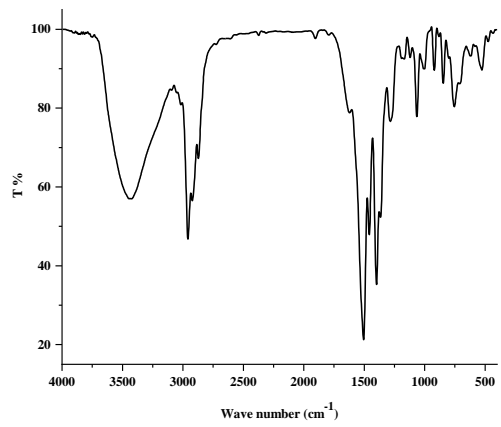


Figure S9: FTIR spectrum of $[\text{Co}(\text{IA})\text{H}_2\text{O}\text{Cl}]\text{Cl}\cdot\text{H}_2\text{O}$.

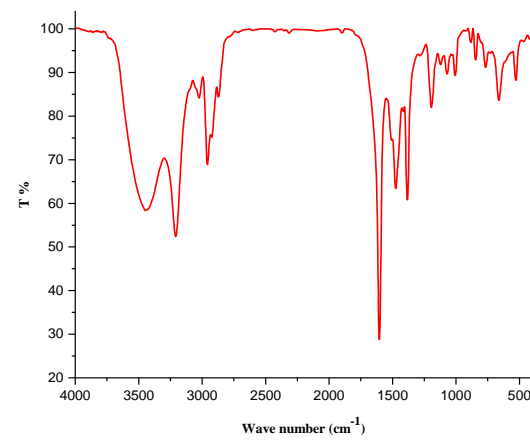


Figure S10: FTIR spectrum of $[\text{Gd}(\text{IA})_2(\text{H}_2\text{O})(\text{NO}_3)]2\text{H}_2\text{O}$.

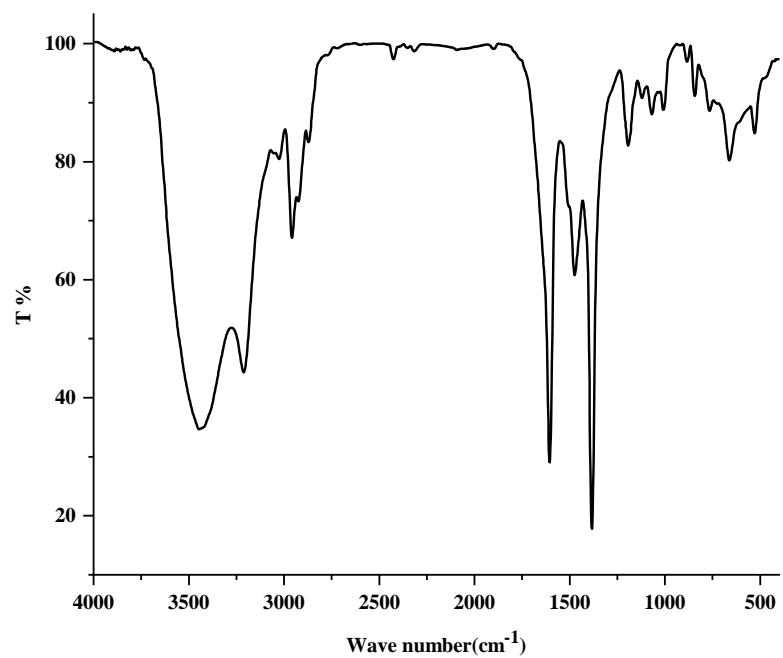


Figure S11: FTIR spectrum of $[\text{Sm}(\text{IA})_2\text{H}_2\text{O } \text{NO}_3](\text{NO}_3)_2 \cdot 2\text{H}_2\text{O}$.

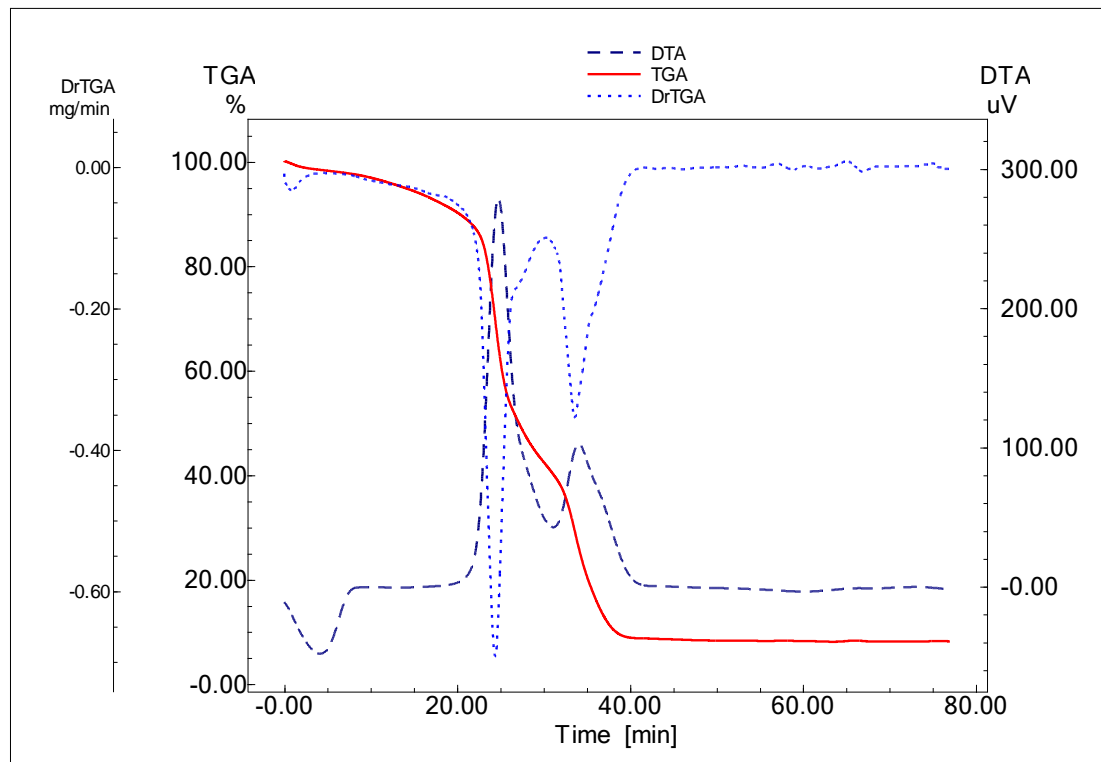


Figure S12: TGA/TG and DTA curves of $[\text{Ni}(\text{IA})(\text{H}_2\text{O})_2 \text{Cl}] \text{Cl} \cdot \text{H}_2\text{O}$ complex.

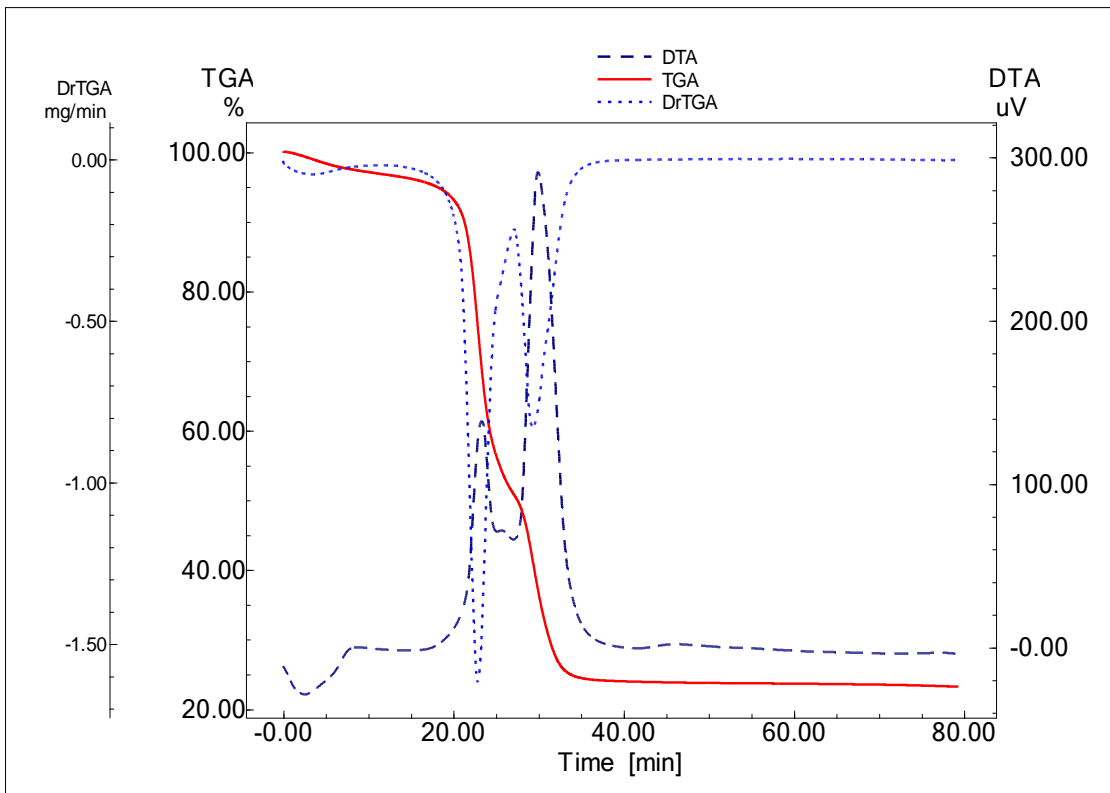


Figure S13: TGA/TG and DTA curves of $[\text{Co}(\text{IA})\cdot\text{H}_2\text{O}\cdot\text{Cl}_2]\cdot 2\text{H}_2\text{O}$ complex.

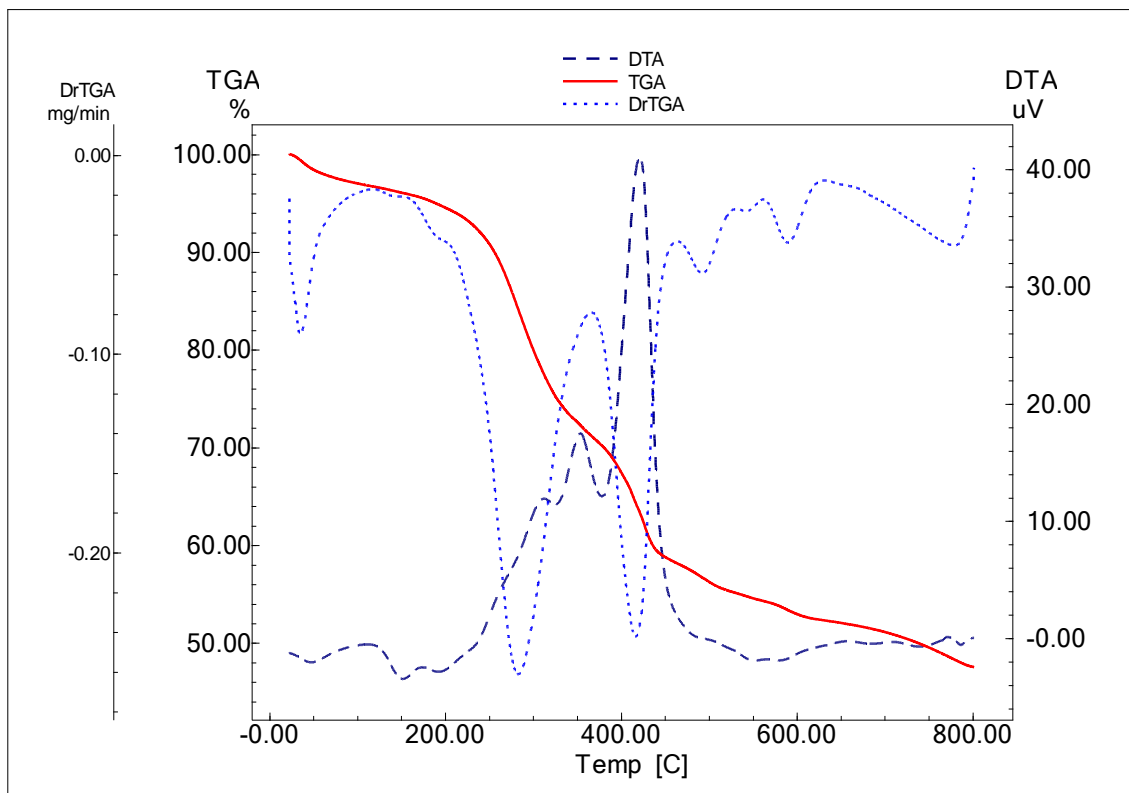


Figure S14: TGA/TG and DTA curves of $[\text{Gd}(\text{IA})_2(\text{NO}_3)_2(\text{H}_2\text{O})]\text{NO}_3\cdot 2\text{H}_2\text{O}$ complex.

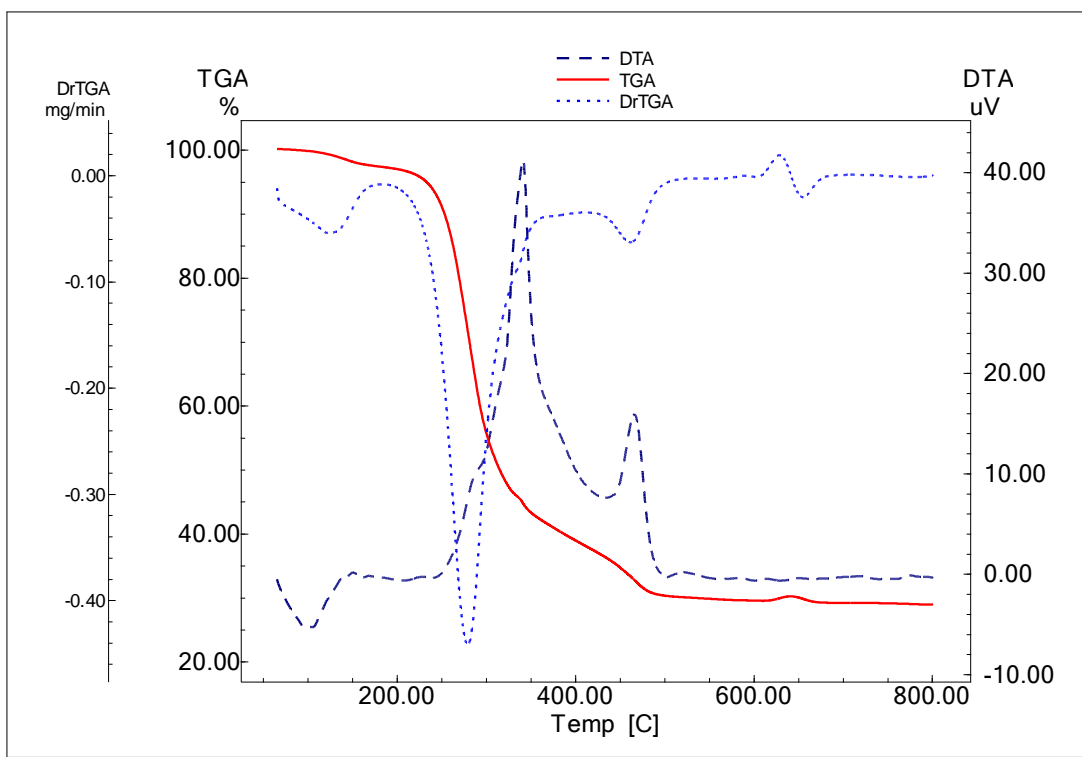


Figure S15: TGA/TG and DTA curves of $[\text{Sm}(\text{IA})_2(\text{NO}_3)_2]\text{NO}_3 \cdot 3\text{H}_2\text{O}$ complex.

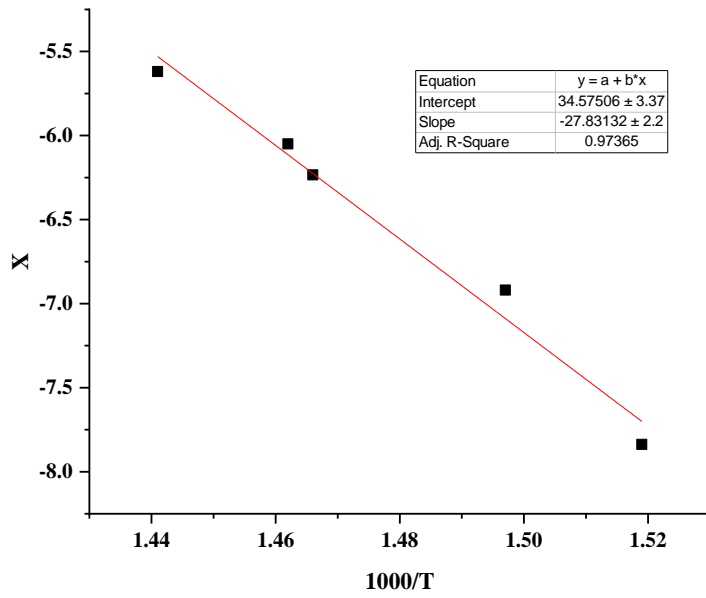


Figure S16: Fit-linear curve of liberation of coordinate water step of **Cu-L2** complex.

Table S3: DTA of Complexes derived from IA Schiff base.

<i>Compound</i>	<i>Temp. range</i> °C	<i>DTA peak temp</i> °C	<i>Peak type</i>	<i>ΔH</i> (kJ/g)	<i>Process</i>
[Cu(IA)(H ₂ O) Cl ₂]6H ₂ O	28-78	56	Endo	0.550	Dehydration
	284-328	308	Exo	-0.851	Coordination sphere+ Partial Ligand decomposition
	341-356	350	Exo	-0.204	Ligand decomposition
	389-437	423,434	Exo	-3.47	Final decomposition
[Ni(IA)(H ₂ O) ₂ Cl]Cl.H ₂ O	46-164	86	Endo	2.29	Dehydration
	289-362	352	Exo	-11.11	Coordination sphere+ Ligand decomposition
	387-437	400,403	Exo	-3.68	Final decomposition
	25-198	46	Endo	0.518	Dehydration
[Co(IA) (H ₂ O) Cl ₂] 2H ₂ O	251-280	273	Exo	-1.26	Coordination sphere+ Ligand decomposition
	319-360	351	Exo	-3.36	Final decomposition
	133-161	48	Endo	0.018	Dehydration
	340-367	352	Exo	-0.382	Coordination sphere+ Ligand decomposition
[Gd(IA) ₂ (NO ₃) ₂ (H ₂ O)] NO ₃ .2H ₂ O	397-445	424	Exo	0.710	Ligand decomposition
	487-510	499	Exo	-0.069	Final decomposition
	56-151	97	Endo	0.050	Dehydration
	330-350	340	Exo	-2.71	Ligand decomposition
[Sm(IA) ₂ (NO ₃) ₂]NO ₃ .3H ₂ O	452-482	466	Exo	-0.234	Ligand decomposition
	510-550	512	Exo	-0.109	Final decomposition

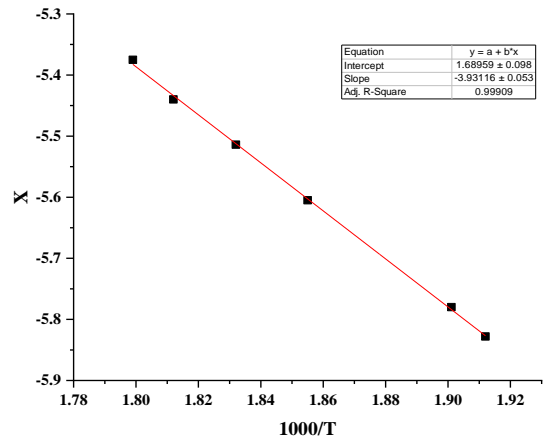


Figure S17: Fit-linear curve of liberation of coordinate water step of **Ni-IA** complex.

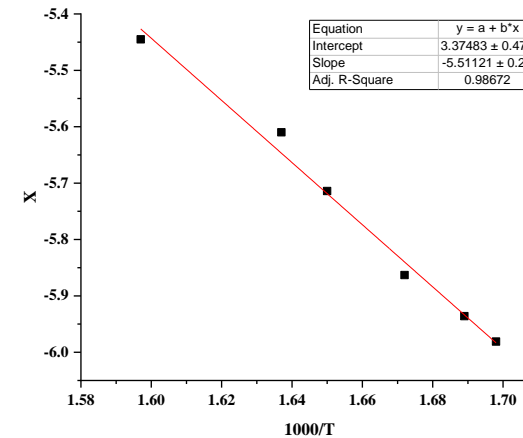


Figure S18: Fit-linear curve of liberation of coordinate water step of **Co-IA** complex.

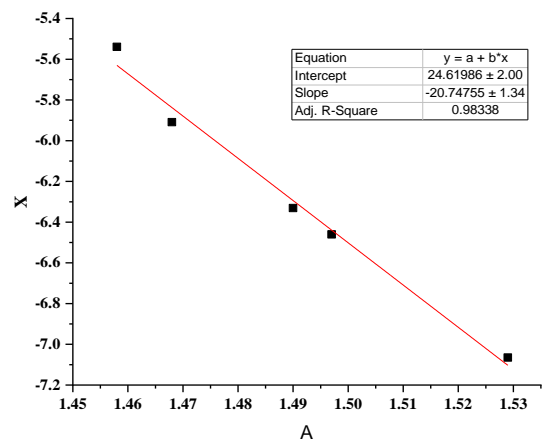


Figure S19: Fit-linear curve of liberation of coordinate water step of **Gd-IA** complex.

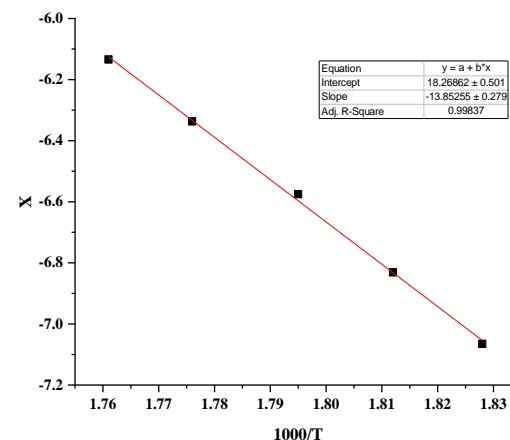


Figure S20: Fit-linear curve of liberation of coordinate water step of **Sm-IA** complex.

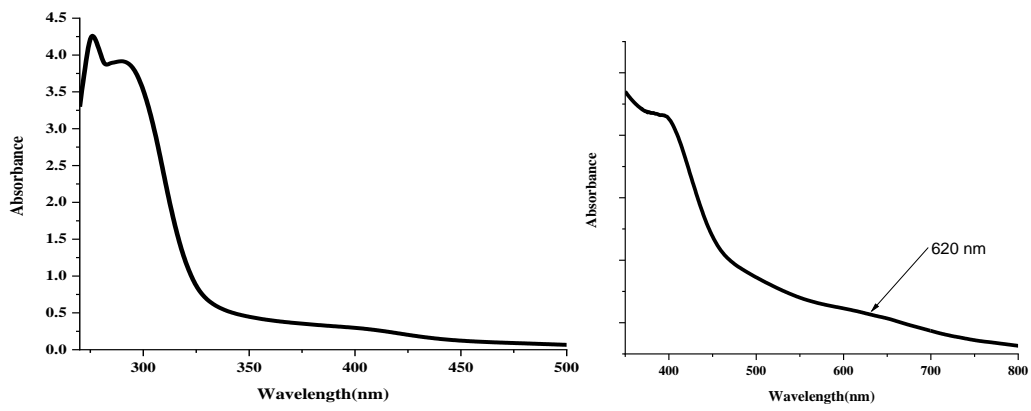


Figure S21: UV-Vis. spectrum of Ni-IA.

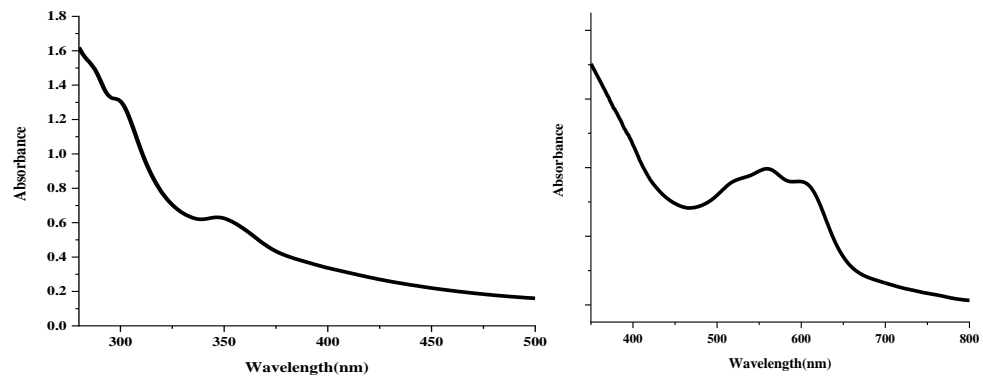


Figure S22: UV-Vis. spectrum of Co-IA.

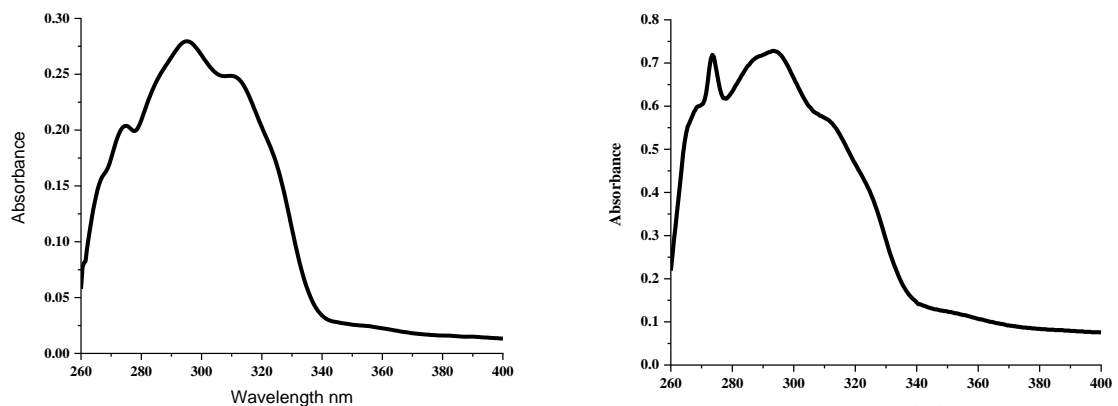


Figure S23: UV-Vis. spectrum of Gd-IA

Figure S24: UV-Vis. spectrum of Sm-IA

Table S4: The magnetic properties and electronic spectra of IA ligand and its complexes

Comp.	Peak		ϵ^* (M ⁻¹ cm ⁻¹) x10 ⁴	Assignment	10Dq		μ_{eff} (B.M)	Postulated Structure				
	nm	cm ⁻¹			cm ⁻¹	kJ/mol						
IA	257	38910	10.34	$\pi \rightarrow \pi^*$	---	---	---	---				
	264	37878	11.27									
	272	36764	10.59	n \rightarrow π^*								
Cu-IA	267	37453	41.28	$\pi \rightarrow \pi^*$	25974	315	2.07	Distorted octahedral				
	280	35714	38.58									
	351	28490	4.30	n \rightarrow π^*								
	385	25974	2.92									
	580	17241	42.53	t _{2g} \rightarrow e _g								
Ni-IA	276	36231	39.16	n \rightarrow π^*	24875	302	2.46	Distorted octahedral				
	290	34482	4.33									
	402	26385	2.92	3A _{2g} \rightarrow 3T _{1g} (P)								
	620	24875	13.18	3A _{2g} \rightarrow 1E _g								
Co-IA	298	33557	6.32	n \rightarrow π^*	16583	201	4.86	Distorted octahedral				
	347	28818	2.79	4T _{1g} (F) \rightarrow 4T _{2g} (P)								
	520	19230	2.98	4T _{1g} (F) \rightarrow 4A _{2g} (F)								
	558	17621	2.78									
	603	16583	2.03									
Gd-IA	275	36363	2.80	$\pi \rightarrow \pi^*$	---	---	8.89	Capped square antiprismatic / Tricapped trigonal prismatic				
	295	33898	2.49	n \rightarrow π^*								
	311	32154	7.14	CT								
Sm-IA	273	36630	7.29	$\pi \rightarrow \pi^*$	---	---	2.29	Bicapped trigonal prismatic / Square antiprismatic				
	293	34129	5.74	n \rightarrow π^*								
	310	32154	10.34	CT								

* ϵ = Absorptivity, 10⁻⁵ M in DMSO, M⁻¹cm⁻¹

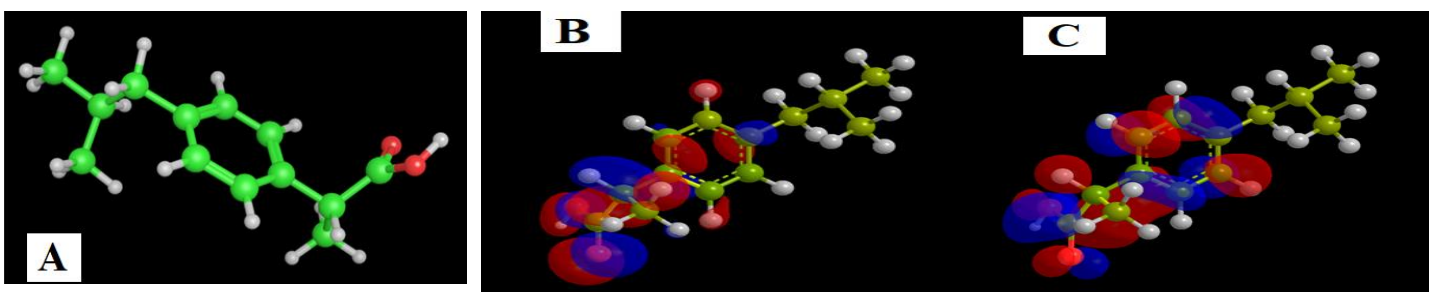


Figure S25: The DFT simulation for the Ibuprofen drug. [A] 3D view, [B] HOMO and [C] LUMO.

Table S5: The DFT simulation data and ligand properties of IA.

<i>Compound</i>	<i>Ibuprofen</i>	IA		
<i>Formula</i>	C₁₃H₁₈O₂	C₁₈H₂₆N₂O₂		
<i>Atoms</i>	33	48		
<i>Orbitals</i>	78	114		
<i>Electrons</i>	82	120		
<i>SCF energy (E_h)</i>	-93.85	-136.49		
<i>Dipole moment (D)</i>	1.94	2.71		
<i>E_{LUMO} (E_h)</i>	0.007	0.009		
<i>E_{HOMO} (E_h)</i>	-0.349	-0.305		
<i>ΔE_{LUMO-HOMO} (E_h)</i>	0.356 (128 nm)	0.314 (145 nm)		
<i>Ionization energy (E_h)</i>	0.348	0.305		
<i>electron affinity (E_h)</i>	-0.007	-0.009		
<i>Absolute electronegativity (E_h)</i>	0.1705	0.148		
<i>Absolute hardness (E_h)</i>	0.211	0.158		
<i>Absolute softness (E_h⁻¹)</i>	5.634	6.369		
<i>Global softness (E_h⁻¹)</i>	2.370	3.173		
<i>Global electrophilicity (ω)</i>	0.045	0.069		
<i>Chemical potential (E_h)</i>	-0.138	-0.148		
<i>Additional electronegativity (E_h)</i>	0.654	0.937		
<i>Toxic.</i>	no	no		
<i>Rsynth (%)</i>	66.67	68.2		
<i>Weight (g/mol)</i>	206.28	302.436		
	37.30	58.53		
<i>TPSA</i>	HD 1	HA 2	HD 1	HA 3
<i>Log p</i>	3.07	3.46		
<i>Log S</i>	-3.64	-4.58		

* **SCF energy:** Self-consistent field, **I:** Ionization potential, **Rsynth (%):** Resynthesized %, **TPSA:**Topological polar surface area, **HD:** Hydrogen donor, **HA:** Hydrogen acceptor, **Logp:** Lipophilicity parameter and **Log S:** Water solubility parameter.

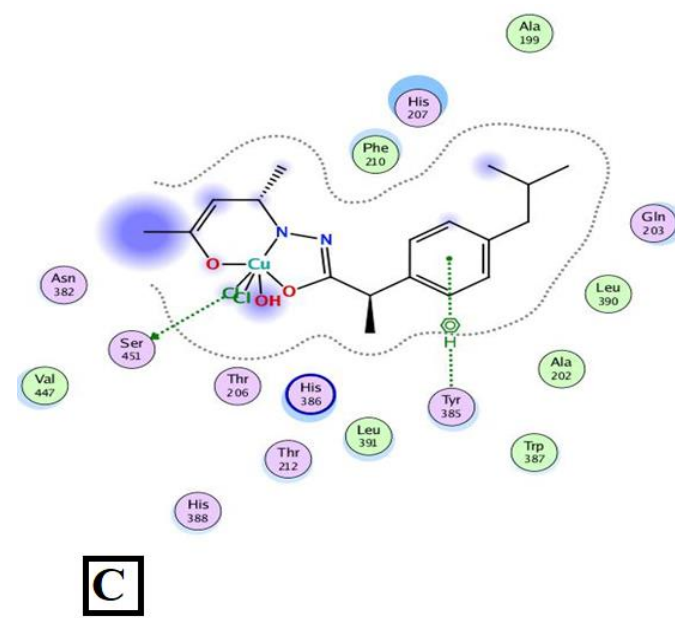
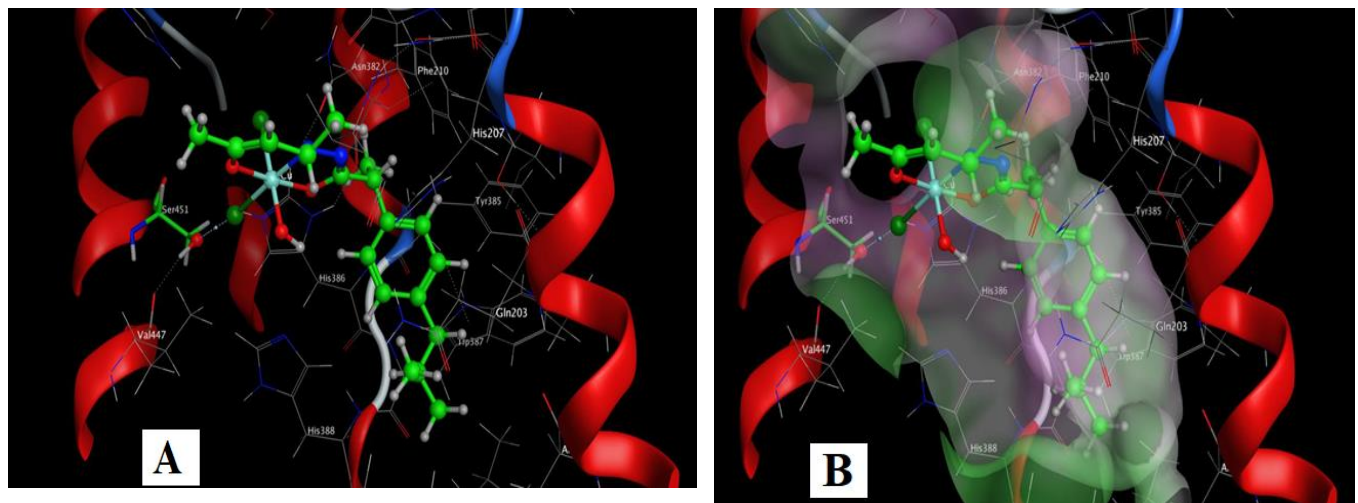


Figure S26: Docking model of the interaction of **Cu-IA** with **Cox2** [PDB code: 5IKT] bonding sites:
 (A) 3D interaction diagram (B) The surface properties [Hydrophilic sites (violet color), neutral sites (white color) and lipophilic sites (green color)]. (C) 2D interaction diagram

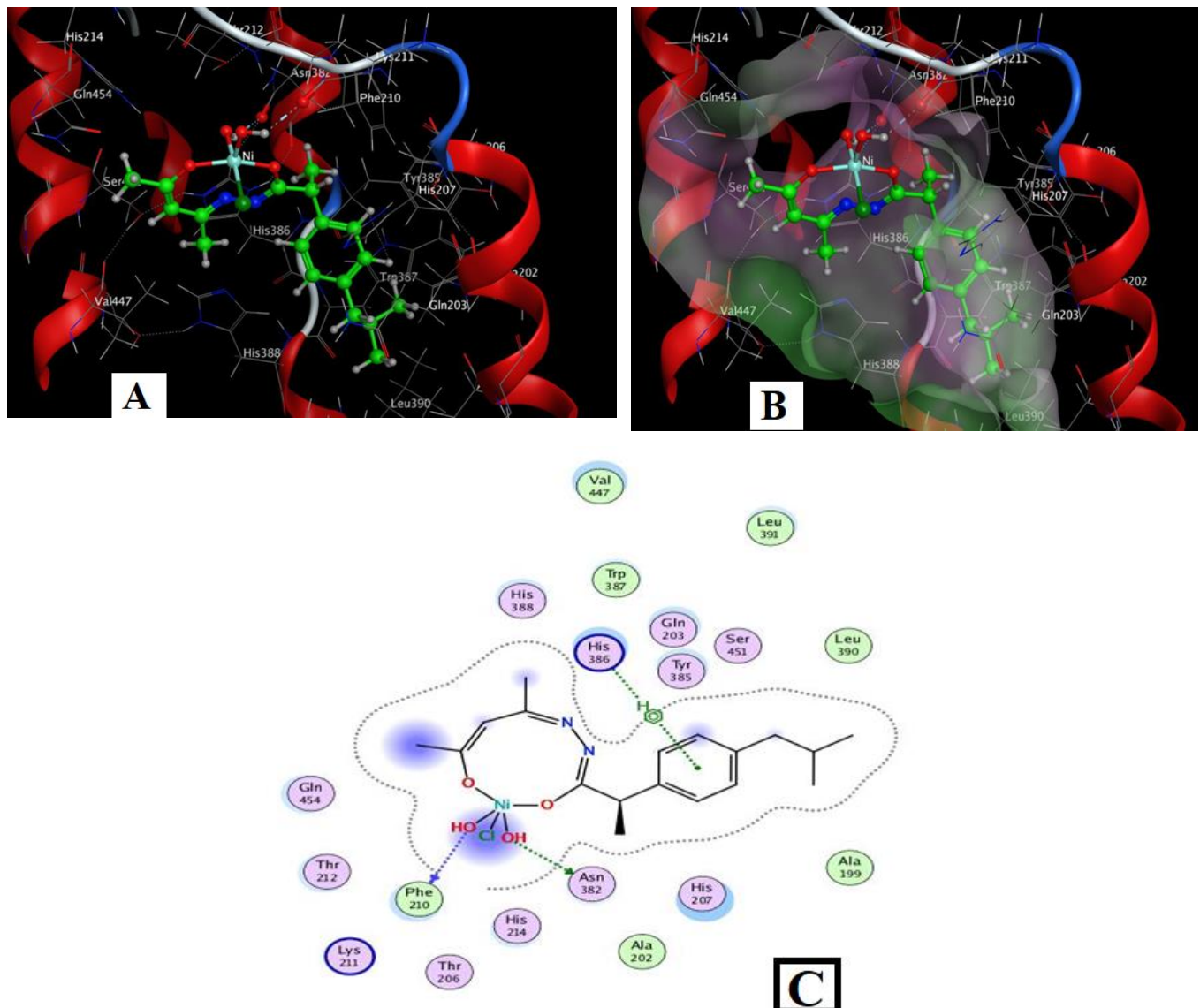


Figure S27: Docking model of the interaction of Ni-IA with *Cox2* [PDB code: 5IKT] bonding sites:
 (B) 3D interaction diagram (B) The surface properties [Hydrophilic sites (violet color), neutral sites (white color) and lipophilic sites (green color)]. (C) 2D interaction diagram

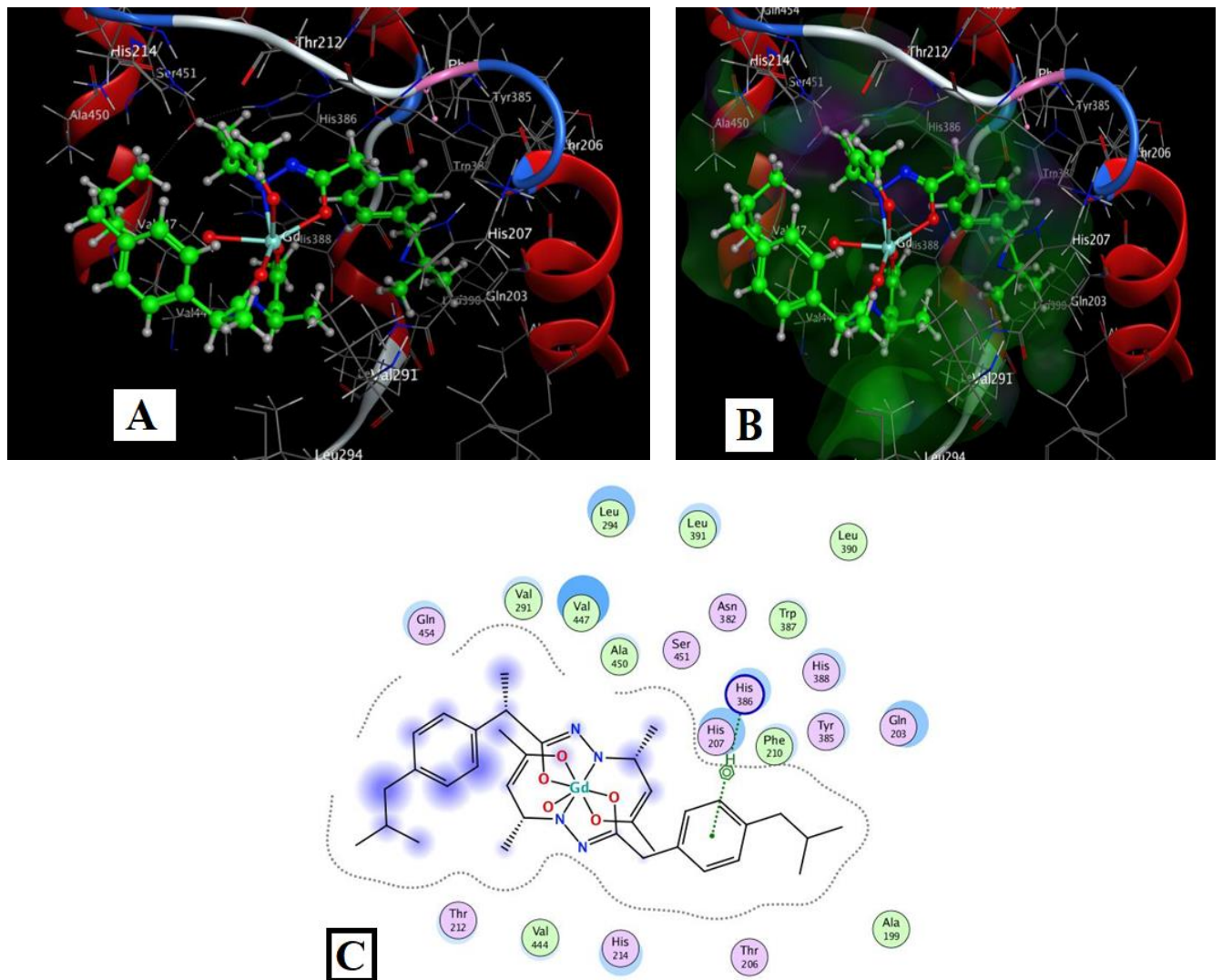
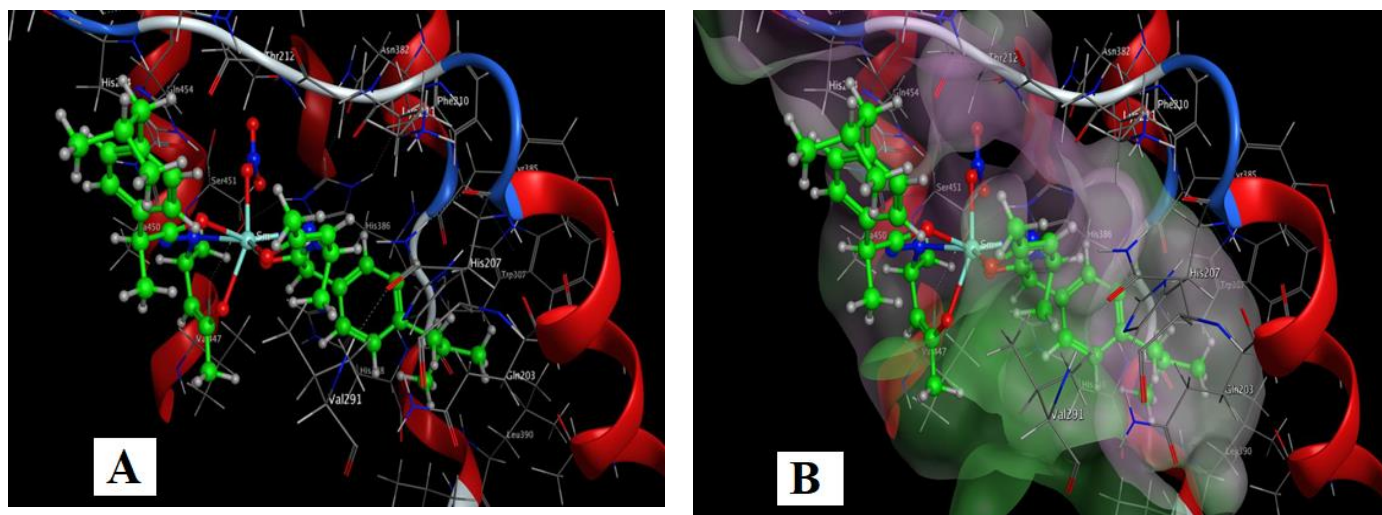


Figure S28: Docking model of the interaction of Gd-IA with *Cox2* [PDB code: 5IKT] bonding sites: (C) 3D interaction diagram (B) The surface properties [Hydrophilic sites (violet color), neutral sites (white color) and lipophilic sites (green color)]. (C) 2D interaction diagram



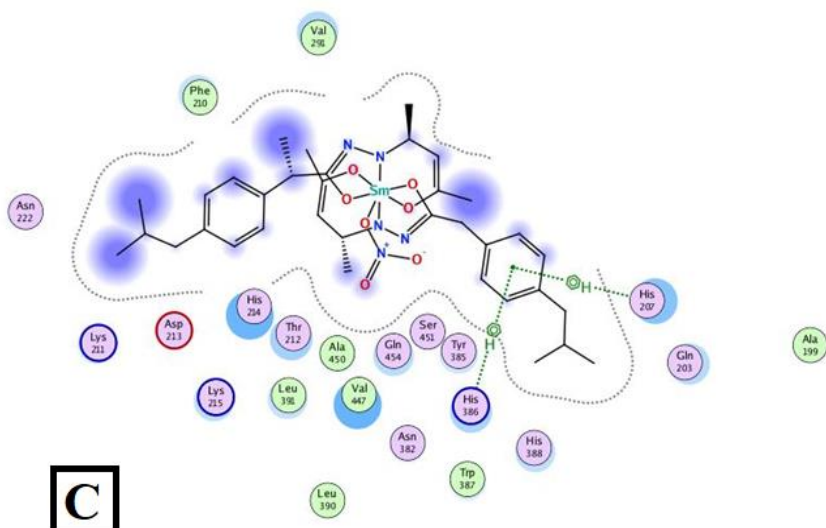


Figure S29: Docking model of the interaction of **Sm-IA** with **Cox2** [PDB code: 5IKT] bonding sites:
(D) 3D interaction diagram (B) The surface properties [Hydrophilic sites (violet color), neutral sites (white color) and lipophilic sites (green color)]. (C) 2D interaction diagram

Table S6: In vitro COX-1 and COX-2 inhibition of different complexes of IA Schiff base.

Compound	IC_{50} COX-2 (μM) ^a
Ibuprofen	31.4
Indomethacin	0.1
Diclofenac sodium	0.8
IA	3.6
Cu-IA	3.4
Ni-IA	2.5
CO-IA	1.6
Gd-IA	2.4
Sm-IA	1.9